NFC-WISP: A Sensing and Computationally Enhanced Near-Field RFID Platform

Yi Zhao
Department of Electrical Engineering
University of Washington
Seattle, WA 98195
Email: yizhao@u.washington.edu

Joshua R. Smith
Departement of Computer Science
University of Washington
Seattle, WA 98195
Email: jrs@cs.washington.edu

Alanson Sample
Disney Research, Pittsburgh
Pittsburgh, PA 15213
Email: alanson.sample@disneyresearch.com

***Abstract*—Near-field radio frequency identification (RFID) tags have a number of unique features such as being wirelessly powered, having ultra low power communication capabilities, small size, and low cost. These qualities paired with the increasing availability of commodity near field communication (NFC) enabled smart phones presents a significant opportunity to enable a wide range of new applications and usage scenarios. However, existing tags are fixed function devices that are only capable of reporting an ID when queried and thus most applications are limited to inventory management or access control.**

This paper presents the NFC-WISP, which is a programmable, sensing and computationally enhanced platform designed to explore new RFID enabled sensing and user interface applications. The NFC-WISP is fully powered and read by commercially available RFID readers (including NFC enabled smart phones) using the ISO-14443 protocol. Excess harvested power can be stored in an optional super-capacitor or thin-film battery enabling operation away from the reader. This open-source platform includes temperature and acceleration sensors, 2MB of FRAM, LEDs and an optional 2.7" active bistable matrix E-ink display. Expansion headers allow access to the microcontroller allowing for rapid prototyping of new applications. The use of the NFC-WISP for a perishable goods temperature and motion monitoring application is demonstrated as well as the use of wireless power transfer based on magnetic coupled resonance for high power recharging of multiple NFC devices.

***Index Terms*—RFID, Near-field, NFC-WISP, Sensors, Wireless Power**

I. Introduction

Near-field Radio Frequency Identification (RFID) technology has achieved wide spread adoption in traditional application spaces such as access control, inventory management, and secure payment [1]. The recent inclusion of Near-Field Communication (NFC) readers in to smart phones has enabled a resurgence in near-field RFID technology with applications focused on human computer interaction, smart living spaces, and healthcare [2]–[4]. With high quality, mobile NFC readers readily available, there is the opportunity to develop new tag hardware with enhanced capabilities to enable further innovation in these application spaces.

At its core near-field RFID tags are wirelessly powered computing devices with basic communication capability, and are activated in the presents of RFID readers. They are small, thin, and low in cost allowing for easy integration into many types of objects used throughout daily life. Although the read range is typically on the order of 1cm to 10cm these tags are able to harvest relatively large amounts of power through inductive coupling compared to UHF RFID tags. However, existing commercially available near-field RFID tags are fixed function devices that only report an ID along with a small payload of data. For many usage scenarios the retrieval of the tags ID is simply a means of obtaining a digital pointer to online content or to activate a user application. Although useful in its own right, the usage metaphor of "tap to activate" is rather limited and does not harness the full potential of the core capabilities of near-field RFID technology.

There are several notable projects that push beyond this simple usage model. Marquardt et. al. [5] describe several ways to add user input and output capabilities to NFC tags in the form of LEDs, vibrating motors, audio beeps as well as touch switches. In all these examples the 13.56MHz RF signal is directly manipulated to provide enhanced functionality rather than using the digital logic inside the commercial RFID ICs. Alternatively, IC manufactures have begun offering NFC chips with a greater range of capabilities [6], [7]. These devices operate as dual interface memory modules where data can be stored and retrieved from non-volatile memory through either a RFID interface or through a microcontroller bus such as I2C or SPI. Although these chips are limited in functionality and fixed to a single protocol when paired with an external microcontroller basic sensing tasks can be accomplished.

In contrast, researchers specializing in integrated circuit design have been able to take full advantage of the capabilities of near-field RFID technology by customizing circuit blocks for peak performance and adding new circuits that extend functionality. One example is a fully implantable, NFC enabled blood glucose monitor [8]. This chip is wirelessly powered through a 13.56MHz inductive link and communicates via an extension to the ISO15693 protocol. On board LEDs and an integrated photo sensor are used to create a fluorimeter which measures blood sugar levels and reports data transcutaneously back to a mobile device. This example shows the potential of near-field RFID technology. However, the process of manufacturing custom integrated circuits presents a significant barrier to entry when considering the high cost of development, chip fabrication, as well as long fabrication cycles.

In order to take full advantage of the unique technology

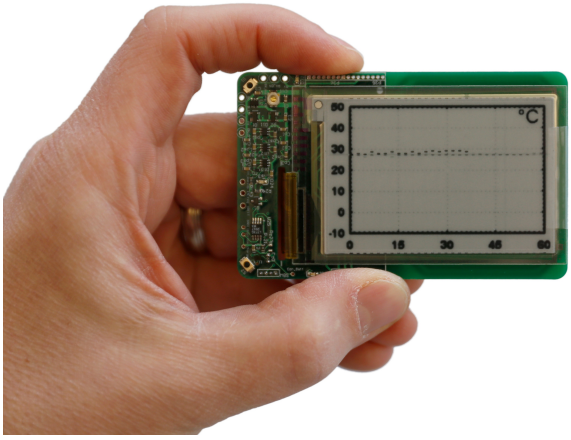

Fig. 1. Image of the NFC-WISP 1.0 with the optional E-ink screen installed.

traits of near-field RFID and to allow researchers to rapidly explore new NFC related applications we present the NFC-WISP (Near Field Communication - Wireless Identification and Sensing Platform), which is shown in Figure 1. The NFC-WISP is a fully programmable sensing and computing platform designed to explore new RFID sensor and human interface applications. At its core it is a software defined RFID tag built around an ultra low power microcontroller (TI MSP430), which handles all the NFC protocol, sensing and I/O tasks in firmware. The NFC-WISP is fully powered and read by commercially available RFID readers (including NFC enabled smart phones) using the ISO-14443 protocol. Extra harvested power can be stored in an optional super-capacitor or thin-film battery enabling operation away from the reader. The platform includes temperature and acceleration sensors, 2MB FRAM, LEDs and an optional E-ink display as well as header pins that interface with the onboard microcontroller for rapid prototyping of new applications.

The NFC-WISP is similar in design and construction to its predecessor the WISP 4.1 DL [9], which for the sake of clarity will be referred to as the UHF-WISP. The key difference is that the UHF-WISP is designed to be a far-field RFID tag operating in the 915MHz ISM band and compliant with the EPC Gen 2 protocol. Another NFC related research effort is the OpenPCD project which has developed a PCB based sniffer tag, but it requires a battery for operation and does not have sensors or display capabilities [10]. Previous work demonstrated the concept of a "Display Tag" which used a E-ink screen as a wirelessly powered, secondary display for smart phones [11]. We extend prior work with a new and more robust hardware and firmware design, as well as a thorough description of the operation and performance characteristics of the NFC-WISP, and demonstrate new applications including: perishable goods temperature and motion monitoring and the use of wireless power transfer based on magnetic coupled resonance for high power recharging of multiple NFC compatible devices.

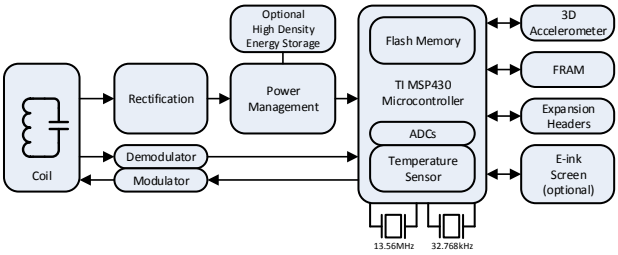

Fig. 2. Block diagram of the NFC-WISP.

II. Hardware Architecture

The NFC-WISP consists of a four layer Printed Circuit Board (PCB) with surface mount components on both sides. The overall dimensions are the same as a standard banking and personal ID card, although slightly thicker ($85.60 \times 53.98 \times 4.8mm$). The near-field antenna is printed on the PCB and consists of a four turn square spiral, with outside dimensions of 42mm by 53mm and a trace width of 1.27mm. Its inductance is 1.2nH and a tuning capacitor is added to make the antenna resonant at 13.56MHz. The matching network is tuned such that the loaded quality factor of the coils when in the presence of the reader is approximately 20, allowing for enough bandwidth to support the 106kbit/s data rate of the ISO 14443 protocol.

A block diagram of the NFC-WISP is shown in Figure 2. The coil antenna and tuning network feed the power harvesting block which rectifies the incoming RF energy into DC voltage to power the system. Since near-field RFID tags receive more power than far-field RFID tags an optional high-density storage element in the form of a battery or super capacitor can be used for long-term storage. The demodulator follows the envelope of the RF carrier wave to extract the amplitude shift-keyed data stream from the NFC-RFID reader. This baseband waveform is read by the TI MSP430F5310 MCU and a 13.56MHz external crystal is used for data recovery. An additional low power and low frequency 32.768kHz watch crystal is used to enable realtime clocking functionality with lower power cost. Uplink data is sent back to the reader from the tag via load modulation. Onboard peripherals such as LEDs, the MSP430s internal temperature sensor, FRAM and an Analog Devices ADXL362 3D accelerometer are powered and managed by the MCU. Finally an optional 2.7 inch Pervasive Display E-ink screen with a resolution of 264×176 ($117dpi$) can be used via the Hirose Electronic's 40 pin ZIF connector.

The primary advantage of the PCB implementation is that it allows designers to quickly and easily modify the hardware and firmware to create new applications. For example if a researcher wants to add a new sensor to the NFC-WISP the exposed header pins allow for easy access to the microcontroller's ADCs and/or digital communication ports (SPI, I2C, or UART). Once the new sensor is added to the NFC-WISP

the microcontroller can quickly be reprogrammed to interface with the new device by using one of the many commercially available and supported IDEs. Finally testing can be done with bench top lab equipment and a JTAG debugger.

III. Energy Harvesting and Power Management

From a power harvesting perspective one of the key advantages of inductive coupling (as compared to far-field energy harvesting methods used on the UHF-WISP) is that the relatively high power levels and the voltage multiplying effect of the multi-turn receive coil means that the NFC-WISP is not inherently voltage constrained. Clearly the system is still power constrained and it must be heavily duty cycled to avoid browning out. However, if the NFC-WISP is placed into sleep mode such that the quiescent current is 9.7μA, it is quite easy to harvest 4-5 volts on the 300μF capacitor bank (or given enough time 4-5volts on the high density storage element). Another way to view this power harvesting optimization problem is to realize that the source resistance of the inductive coupled system is typically much lower than in far-field systems.

Figure 3 panel A shows a detailed block diagram of the power management circuitry. A three-stage full wave rectifier is used to convert the 13.56MHz RF wave into un-regulated DC voltage, which is stored on a 300μF bank of ceramic capacitors. A 5.6v Zener diode is used to provide over voltage protection. The unregulated power is passed to a 2.5v linear regulator, which was chosen for robustness, fast start up time, and low headroom. When the rectified voltage is under the 2.5v threshold the linear regulator stays open and passes unregulated power to the system. Under most circumstances the NFC-WISP can harvest more power from the reader than it consumes (a detailed analysis of power consumption is presented in section VI). This power can be stored in an optional high density storage device for use with high current peripherals or for prolonged sensing and computing tasks were the NFC-WISP must operate away from the RFID reader.

The LTC4071 shunt battery charger was chosen since it is a linear trickle charger that does not induce switching noise on its $V_{Rectified}$ supply line. Additionally, the LTC4071 provides a simple two pin interface (power and ground) and current can flow bidirectionally, mimicking the functionality of a large capacitor. When extra charge storage is needed either a thin-film battery such as the Power Stream 30mAh, 3.7V PGEB014018 or a super capacitor such as the Kanthal 0.1F LX055104A can be used. If the use of a battery is not needed, the user can easily disable the charger IC in the hardware.

Figure 3 Panel B shows a conceptual diagram of the operating points of the NFC-WISP based on the rectified voltage. Assuming the system starts from a cold start (i.e. $V_{Rectified} = 0v$, when the NFC-WISP is with in range of a RFID reader the rectifier will start storing charge on the 300uF capacitor bank. When the rectified voltage reaches 4.2V the main supervisor block enables the 2.5v linear regulator and the system begins operating.

If a thin-film battery or supercap is installed, the supervisor will also enable the LTC4071 at 4.2v. It should be noted that once the LTC is enabled the $V_{Rectified}$ node will essentially be "pegged" at the operating voltage of the charge reservoir. This means that it may take a long period of time to charge up the battery / supercap. However, passive operation is guaranteed since the LTC4071 will disconnect itself from the system at 2.7v, thus leaving 2.7v of charge on the 300μF capacitor bank which is enough energy for passive RFID reads and simple sensing task. As a point of reference the storage cap on the UHF-WISP is only 10μF.

As power is consumed the stored voltage will decrease resulting in a number of warning signals and ultimately the shut down of the system. At 2.3v a second supervisor warns the MSP430 that stored power is limited and is below the minimum voltage requirement for updating the E-ink display. At 1.8v the main supervisor block disables the linear regulator and the system is power down to avoid the MCU entering a prolonged and uncontrolled brown-out state. The NFC-WISP also includes a voltage measurement circuit consisting of a pass transistor network and a voltage divider. Thus, at anytime the MSP430 can measure the rectified voltage to determine if there is enough stored charge to complete a given task.

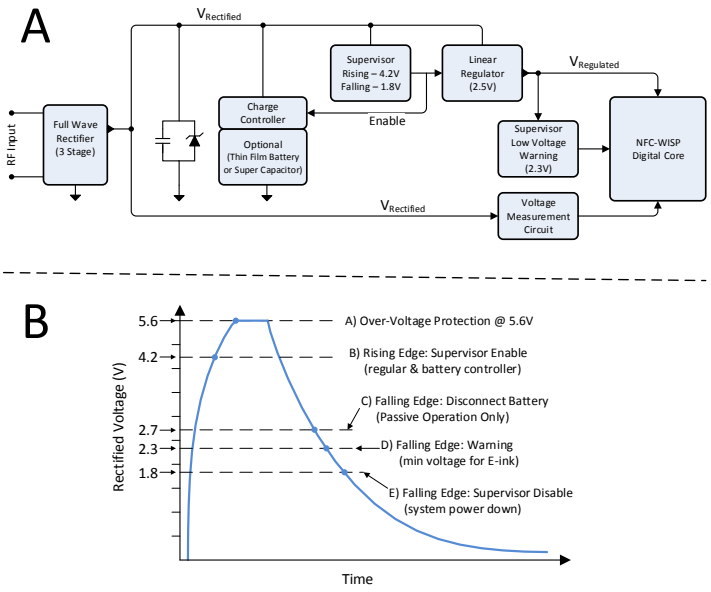

Fig. 3. Panel A shows a detailed block diagram of the power management circuitry along with optional thin-film battery or super-capacitor. Panel B shows activation thresholds based on harvested power.

IV. Demodulation, Data Recovery, and Load Modulation

The task of demodulating and interpreting the amplitude modulated data from the RFID reader, is particularly challenging given the limitations of discrete components and an off-the-shelf microcontroller. Thus, the power consumption and timing constraints of the MSP430 must be carefully considered

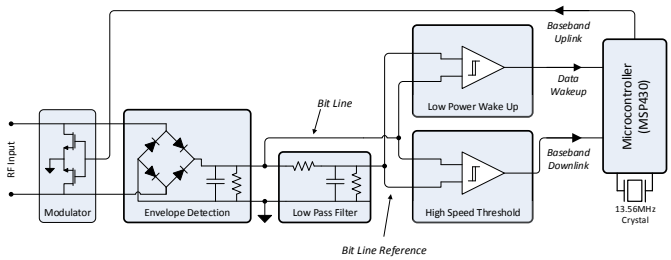

Fig. 4. Simplified circuit diagram of the demodulation and data recovery blocks, along with wake up and load modulation circuitry.

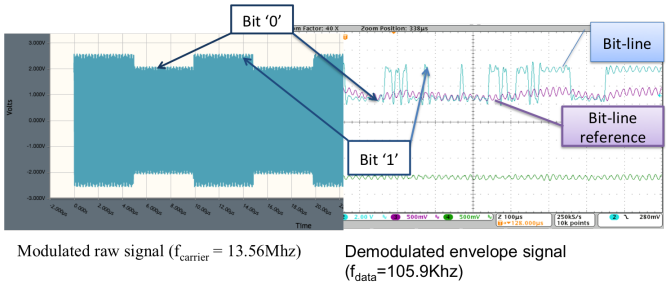

Fig. 5. The right panel shows ASK modulated data from the RFID reader. The left panel shows the demodulated envelope labeled "Bit Line" and the average amplitude labeled "Bit Line Reference". These two signals are sent to the high speed comparator for thresholding.

so that the system does not "brown out" when operating in fully passive (i.e. battery free) mode.

Figure 4 shows a simplified circuit diagram of the analog front end of the NFC-WISP. It has been designed to demodulate both the ISO-15696 (1:256 & 1:4) protocols as well as the ISO-14443 (A & B) protocols. However, at the time of this publication only the ISO-14443B protocol has been fully implemented in firmware on the MSP430. Returning to Figure 4, the raw RF signal from the antenna is fed into an envelope detector which consists of a single stage full wave rectifier. The resulting signal is shown in Figure 5 and is labeled "Bit Line".

One challenge is that the ISO-14443 Type-B protocol uses 10% carrier modulation depth as apposed to both ISO-14443A or EPC Gen 2 which both use a modulation depth of 90% or greater. This means that once the RFID signal from the reader is demodulated, the data symbol difference on the "Bit Line" (that is the voltage difference between symbol "1" and symbol "0") is typically between 2mV to 20mV. Further complicating the task of bit recovery is that the DC bias level of the "Bit Line" changes as a function of RF input power (i.e. reader to tag distance), and fluctuations in the system load can cause low frequency load modulations that ripple back to the antenna and can also change DC bias points.

To overcome these challenges, a low pass filter is used to track the mean amplitude of the "Bit Line". This signal is shown in Figure 5 and is labeled as "Bit-line Reference". These two signals ("Bit Line" and "Bit Line reference") are sent to a high speed comparator which thresholds and level shifts the data so that in can be interpreted by the MSP430. Since the quiescent current draw of the high speed comparator is $\sim$10uA, it is power gated by the MSP430 and only used when demodulating data from the reader. The rest of the time the low power (and lower speed) comparator is used to wake up the system when RFID data is detected. The low power comparator consumes $\sim$10nA of current and the complete NFC-WISP consumes 9.7μA of current when in low power sleep mode.

Both the ISO-15693 and ISO-14443 protocols are designed to allow the RFID tags to use the 13.56MHz ($\pm 7kHz$) RF carrier as a clock for their digital logic blocks. Additionally the data transmitted from the reader to the tag, has timing requirements such that the symbol rate = carrier frequency / 128. This has two important implications for conventional tag design: 1) the tag does not have to use extra power or die space for clock generation circuitry, and 2) recovering the timing of the data signal (i.e. data clock) is implicit in the protocol making data recovery a much simpler task. Essentially a normal NFC tag can simply use a timer, that is clocked by the RF carrier, to record the time interval between data edges in order to recover the raw bits.

In contrast the NFC-WISP uses an external 13.56MHz crystal as a clock source when communicating with the reader, instead of the RF carrier itself. This architectural choice was made to avoid the potential of a corrupted "RF clock" halting code execution on the MSP430. A further decoding challenge imposed by the discrete analog-front-end is that the bit width is not always constant as a function of input power due to the RC time constant of the envelope detector. Also small shifts in the symbol rate occur since it is tie to the carrier frequency which can deviate $\pm 7kHz$ from 13.56MHz.

To address these issues and increase the timing tolerance, a new interrupt based data recovery subroutine has been implemented on the MSP430 using a mixture of assembly and C. In this approach the the 13.56MHz clock generated by the crystal is divided by 8 and used to clock Timer A. The MSP430 is placed into sleep mode (LPM3) and a wakeup interrupt is set on the demodulated data edges from the high speed comparator. When triggered the interrupt routine starts/stops the timer and compares its values to expected thresholds for 0 and 1 bits. Although this approach results in a small increase in power consumption as compared to the previous method [11], it significantly increase the robustness and usability of the platform as the timing tolerance is increased by $\pm 30\%$

Communication from the NFC-WISP to reader (the uplink) utilizes BPSK (Binary Phase Shift Key) load modulation. Two uplink transistors are controlled by the MSP430 to encode NRZ-L data on a 847.5 kHz load modulated subcarrier. Since the NFC-WISP can generate fully custom data packets in software, data can be sent to the reader as part of the tags ID or as part of the read command.

V. Firmware

The firmware of the NFC-WISP is optimized for minimum power consumption and as such the system is heavily duty cycled. Figure 6 depicts the firmware state diagram implemented on the NFC-WISP. After the NFC-WISP is powered up from a cold start, all communication functions and user applications are initialized and the NFC-WISP will enter a NFC reading waiting sleep mode. In this sleep mode, only the 13.56MHz crystal and the wake-up comparator mentioned in IV are enabled, other hardware peripherals are either disabled or put into standby mode. The MSP430 in NFC-WISP waits for an interrupt from the low power wake-up comparator indicating that NFC traffic is present. If valid NFC data is detected, the system enters the NFC event handler routine which interprets ISO-14443 Type-B commands sent from the RFID reader, formulates packets, and responds back to the reader via load modulation. Any other tasks or interrupts required for user applications are either disabled or blocked to avoid interfering with NFC communication.

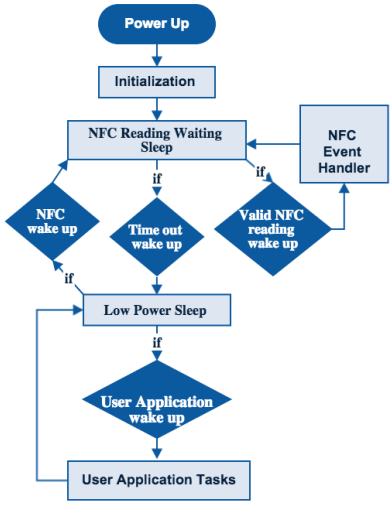

Fig. 6. Firmware diagram with API interface.

However, if no NFC traffic appears within a pre-defined timeout, the NFC WISP will enter a low power sleep mode in which the 13.56MHz crystal is disabled to further save power. All interrupts from either the wake-up comparator or user applications are enabled in this mode. Typically, user applications are heavily duty cycled to conserve power. Sleep functionality is handled by the user application which allows the programmer to specify wakeup intervals and events. Once in this low power sleep mode, the system can either be woken up by NFC traffic interrupts from the low power comparator or by the applications. In order to simplify programming tasks for the users, the application function is decoupled from the NFC communication. As such while the application task are running, all NFC communication interrupts are halted until the system returns to the low power sleep state. If NFC traffic wakes up the system in this low power mode, it will enable and stabilize the 13.56MHz crystal and jump into the previous NFC reading waiting sleep mode to further decode the NFC commands.

Note that all data can be passed between the application and NFC event handler via a data structure that can be stored in SRAM or non-volatile memory. The RFID reader or cell-phone can also send commands directly to the application space triggering actions such as configuring sensing tasks, taking sensor readings, preparing data for off load or updating the E-Ink screen.

VI. Performance and Measured Results

The NFC-WISP's read performance and power harvesting characteristics were tested using the Texas Instruments TRF7970A evaluation board and the Nexus 5 smart phone (which uses Broadcom's BCM20793M NFC controller). The TI NFC reader is configured to repeatedly query the NFC-WISP using the REQB command at a known peak power level of $200mW$. The Nexus 5 smart phone allows for a more real world testing scenario but offered limited control over the NFC communication. The "NFC Research Lab" Android application was used to read the NFC-WISP. In this case it was observed that the Nexus 5 continuously scanned for tags using multiple NFC protocols at an unknown output power level.

The results for passive read range (without a battery) and semi-passive read range (with a 30mAh thin-film battery) are shown in Table I. Since the NFC-WISP operates in a duty cycled fashion it can take several read cycles to harvest enough voltage for tag operation. In passive mode charge up time is less than a second and the latency is not apparent to the user. As described early, if there is not enough charge on the battery in semi-passive mode the NFC-WISP defaults to passive mode. It should also be noted that the read rate and tag alignment are more robust in semi-passive mode since the presence of the battery stabilizes load current pulses which can corrupt the demodulator signal.

Table I also shows the amount of excess current that can be harvested (at 3.7V) for different operating modes. In this test the tag was place directly next to or on the reader to show the maximum amount of harvestable current. Clearly, if the tag is place at its maximum read distance no excess current will be available for harvesting. It should be noted the polling rate of

TABLE I
NFC Reading and Harvesting Performance

Category	Reader Type	Value
Read Distance: Passive Mode	TI NFC reader	3cm
	Nexus 5	0.5cm
Read Distance: Semi-Passive Mode	TI NFC reader	11.5cm
	Nexus 5	1.2cm
Extra harvested current: Sleep Mode	TI NFC reader	4mA
	Nexus 5	1.9mA
Extra harvested current: Read Mode	TI NFC reader	3.7mA
	Nexus 5	1.65mA

TABLE II
NFC WISP POWER CONSUMPTION

Category	Power Consumption	Duration
Sleep/Charging Mode(disable FRAM)	9.7μA*	N/A
Sleep/Charging Mode(enable FRAM)	12.7μA	N/A
Demodulation(REQB command)	2.6μJ	783μs
Modulation(ATQB command)	11.4μJ	1.6ms
E-ink Update(1 frame cycles)	8.1mJ	0.57s
E-ink Update(4 frame cycles)	9.72mJ	0.98s
Accelerometer (single sample)	267nJ	45μs
Temperature sensing (single sample)	369nJ	94μs
Temperature sensing and single line E-ink update	3.6mJ	0.57s

*Quiescent current draw

the reader significantly effects the amount of average power that is transferred to the tag, while peak reader power is most useful for increasing tag read range.

The energy consumption of the NFC-WISP for different tasks is shown in the Table II. In Sleep Mode (which is also used for Charging Mode) the MSP430 goes to sleep and all peripherals such as FRAM, accelerometer, and E-ink screen are placed into standby mode as described in section V. The average transmit and receive power consumption for a ISO-14443B communication round is also shown. A detailed screen shot of the demodulation and modulation power consumption is shown in Figure 7. Here the demodulated REQB command from the reader is shown in blue (labeled: RX) and the tags ATQB response packet is shown in purple (labeled: TX). Real time power consumption is plotted in red (labeled: Power). The energy consumption of other tasks depends on the peripherals used and how they are configured. A few examples such as temperature sampling and accelerometer measurements are reported in table II.

The new generation of E-ink screens from Pervasive Displays uses a new driver that reduces the power consumption and update time compared to our previous work [11]. It is useful to remember that E-ink technology is bi-stable meaning that the image remains without consuming any active power. Thus, the power consumption numbers reported are for changing the image on the screen. The quality of the updated image on the E-ink display depends on how many times the new image is loaded to the screen (referred to as frame cycles). If only one frame cycle of a new image is applied, ghosting of the old image can remain. Thus more frame cycles will improve the new image quality but will also increase the energy cost. Additionally, individual lines of the E-ink screen can be updated greatly reducing power and update time. This is particularly useful when updating a plot of sensor data since most of the screen will remain the same.

VII. APPLICATIONS

The NFC-WISP is a programable NFC tag and has an ultra-low power display, large data storage, as well as computing

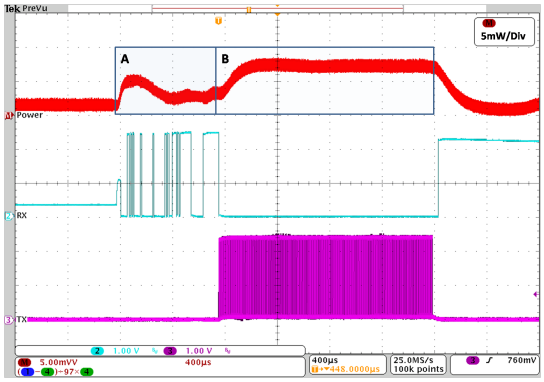

Fig. 7. Power consumption of NFC communication: The red line is the overall power consumption of the system during NFC demodulation and modulation. It is obtained by measuring the voltage across a 97Ω resistor which is series connected to the power supply feeding the system. The blue line (RX) is the demodulated digital signal(bit rate is $105.9kHz$, it is decoding the 5 bytes REQB (including CRC bytes) command in the figure), the purple line (Tx) is the modulated digital signal (bit rate is $847.5kHz$), it is responding 14 bytes ATQB (including CRC bytes) to the reader. The block A represents the period of demodulation, and block B refers to the period of modulation.

and sensing capability. A user can either create customize applications using current hardware or add other peripherals through the extension headers to add new functionality to the base platform. Below we introduce some application examples which use the stock NFC-WISP hardware.

A. Cold Chain Data Logging

Below,we demonstrate the use of the NFC-WISP as a data logger and display for a cold chain monitoring application. Since the tag needs to operate away from the RFID reader a high density storage device (in the form of a $30mAh$ thin-film battery) is included as shown in Figure 8 panel A. Panel B shows the NFC-WISP mounted to a milk container with the optional E-ink screen included. It should be noted that the E-ink screen does not have any noticeable effect on the performance of the coil antenna. In this experiment the milk container is sent on a simulated shipment around our office; and temperature, 3D orientation, and motion events are recorded. Once the container and tag is returned to the RFID reader, the recorded data is downloaded via a RFID interface to a host computer for post processing. Additionally, the latest 30 temperature samples are displayed on the E-ink screen. The temperature and 3D acceleration sample intervals can be modified in software, here it is configured for 5 seconds for demonstration purposes.

The operation of the NFC-WISP is similar to the UHF RFID based passive data logger described in [12], [13]. The key difference is that the NFC-WISP allows personnel to both download the food temperature history using a NFC enabled smart phone, as well as visually check the E-ink screen. This is important in cold chain monitoring applications where a person can immediately see the temperature history of a product and can take immediate steps to prevent further food born contamination down the line, rather then waiting for post processing needed for typical data loggers.

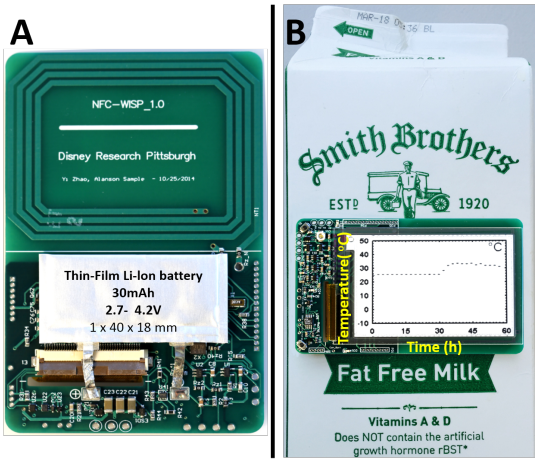

Fig. 8. Image of a NFC-WISP configured with the E-ink display and rechargeable thin-film battery for monitoring and displaying the temperature of milk, in an example cold supply chain monitoring scenario.

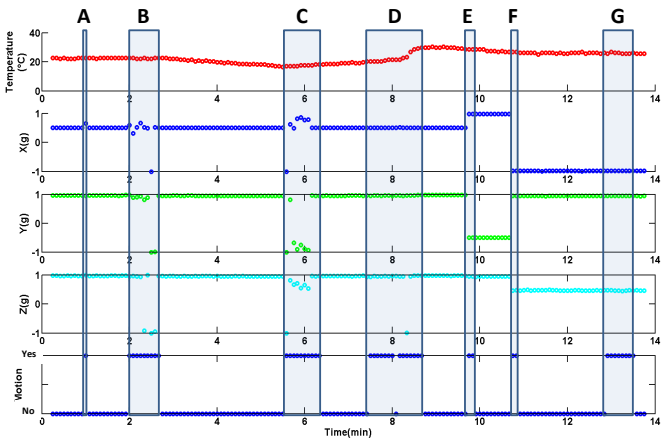

Fig. 9. Data collected by the NFC-WISP operating in semi-passive mode while monitoring a milk carton.

The data collected by the NFC-WISP data logger is shown in figure 9 which depicts the temperature, 3-axis acceleration, and motion events recorded by the tag over a 15min period. The sampling rate for the temperature and 3-axis acceleration data was 5 seconds and was stored in the internal flash memory on the MSP430. Future implementations could take advantage of the 2MB onboard FRAM chip to increase the record length. Additionally, the ultra low power motion detection functionality of the ADXL362 was enabled to detect the motion from subtle vibrations to large movements.

As a point of reference figure 9 also shows scripted event labels highlighted in light blue. Events A, E, F and G show motion events and changes in orientation, which are correctly detected by the plots of the X, Y, and Z acceleration data and the motion detection plot. During event B the milk carton was placed in a refrigerator and cooled until it was removed at event C. During event D the milk carton was heated with a hair dryer to simulate a temperature increase that would be seen during transport. Finally, when the experiment was completed the NFC-WISP is place back on the reader and the data is downloaded to a host PC.

B. NFC RFID + WPT Magnetic Coupled Resonance

One of the key benefits of near-field RFID technology is the ability to wirelessly transfer power from the reader to the tag. Commercially available RFID readers are limited to an output power of 100mW to 200mW due to the modulation of the uplink and downlink data as required by FCC part 15 [14]. However, if data is not modulated on the RF carrier, FCC part 18 [14] regulations state that the permissible output power is unlimited as long as health and safety limits are met in terms of Specific Absorption Rate (SAR).

Recent work on magnetic coupled resonance has shown the ability to transfer 10s of watts, at greater than 80% RF to RF efficiency, over medium distances, in uncontrolled and dynamic environments. This type of wireless power is best suited for the 1-30MHz range and many systems have converged on the 13.56MHz ISM band. Additionally, recent work by Christ et. al. [15] has shown the wireless power transfer based on magnetic coupled resonance can transfer as much as 45-280 Watts (for certain coil configurations) before SAR limits are met. This suggest that it is possible to merge NFC RFID technology with wireless power technology to produce a hybrid solution that can communicate and send low amounts of power in “RFID mode” and then send large amounts of power in “wireless power only mode” to enable fast and multiple device recharging.

A prototype system is shown in Figure 10 which depicts four NFC-WISPs being charged wirelessly by a magnetic resonator, with the drive coil and RF amplifier under the table. The wireless power system used is described in detail in [16]. Although the two systems share the same physical layer based on the 13.56MHz ISM band there are significant differences in the near-field coil design and tuning that effects wireless power transfer efficiency. Near-field RFID coils are optimized

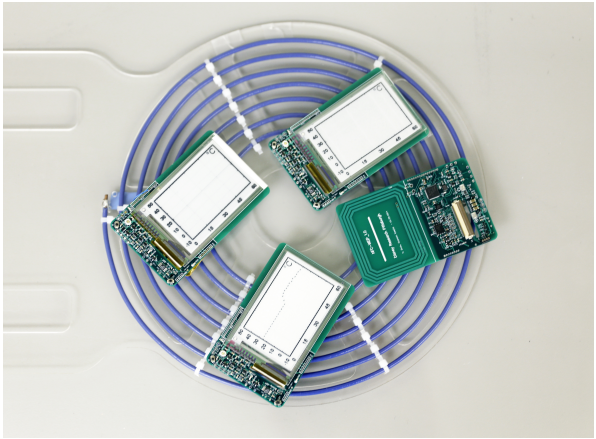

Fig. 10. Image of four NFC-WISP placed on a magnetically coupled resonant charging coil.

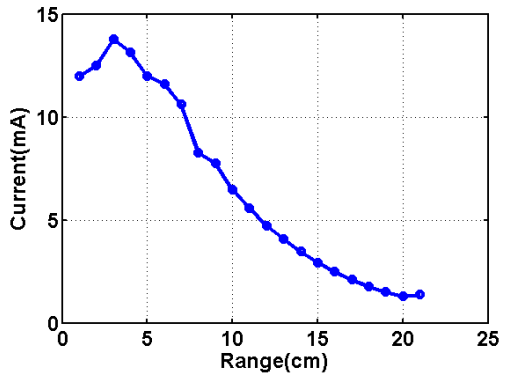

Fig. 11. Plot showing the amount of current that can be harvested from the wireless power transmitter as a function of distance.

for data transfer resulting in the need for a higher bandwidth link and thus a relatively low quality factor, typically around 20 to 30. This is opposed to high power Magnetically Coupled Resonators (MCR) systems that operate on a single tone and use coils with a quality factor of 100 to 300. The result is that when low Q coils, such RFID tag coils, are used in MRC it is difficult for the combined system to enter the over-coupled regime and optimal power transfer may not be possible.

The NFC-WISP was placed into sleep mode and the rectified current delivered to the $10mAh$ thin film battery was recorded. The Wireless Power (WP) transmitter was set to output a single 13.56MHz tone at 1Watt. The tag was then moved towards the transmitter such that the center of the WP transmitter's coil and the NFC-WISP's coil are aligned. Figure 11 shows a plot of harvested current as a function of distance from the WP transmitter. The plot shows that as the NFC-WISP is brought closer to the WP transmitter the amount of current that is delivered to the thin-film battery increases till 4cm when the system becomes over-coupled and the amount of current decreases. It should be noted that the charging current was limited to approximately 10mA to protect the battery.

VIII. Conclusion

This paper describes the design of the NFC-WISP which is a reconfigurable platform designed to explore enhanced near-field RFID tags and applications. The platform is compatible with the ISO-14443B protocol and works with wired near-field readers and NFC enabled smart phones. A number of sensors and peripherals have been included into the design including temperature, 3D acceleration as well as LEDs and FRAM. To the best of the authors' knowledge the NFC-WISP is the first passive and/or semi-passive RFID tag which includes an active metrics bi-stable E-ink screen that is completely powered from harvested power. Additionally we show that the NFC-WISP can be used for cold chain monitoring applications, as a RFID data logger, and provide immediate temperature history to personnel without the need for post processing via the E-ink screen. Additionally, the use of magnetically coupled resonant wireless power transfer is demonstrated for recharging multiple NFC-WISPs.

Furthermore, this paper argues that the NFC-WISP can fundamentally lower the barrier of entry to RFID research and will allow people from a wide variety of fields to develop new and innovative near-field RFID applications. Whether it is students, security specialists, consumer electronics designers, or artists, it is believed that a diverse group of people will be able to push RFID technology and find new and useful usage models. The hope is that this will lead to the discovery of compelling applications and that IC tag designers will be able to draw upon the lessons learned from the NFC-WISP. As such the NFC-WISP has been open-sourced and all design files and example code can be found online [17].

References

[1] S. Ahson and M. Ilyas, *RFID handbook : applications, technology, security, and privacy*. Boca Raton: CRC Press, 2008.

[2] G. Broll, E. Rukzio, M. Paolucci, M. Wagner, A. Schmidt, and H. Hussmann, "Perci: Pervasive service interaction with the internet of things," *Internet Computing, IEEE*, vol. 13, no. 6, pp. 74–81, Nov 2009.

[3] M. Darianian and M. Michael, "Smart home mobile rfid-based internet-of-things systems and services," in *Advanced Computer Theory and Engineering, 2008. ICACTE '08. International Conference on*, Dec 2008, pp. 116–120.

[4] E. Freudenthal, D. Herrera, F. Kautz, C. Natividad, A. Ogrey, J. Sipla, A. Sosa, C. Betancourt, and L. Estevez, "Suitability of nfc for medical device communication and power delivery," in *Engineering in Medicine and Biology Workshop, 2007 IEEE Dallas*, Nov 2007, pp. 51–54.

[5] N. Marquardt, A. S. Taylor, N. Villar, and S. Greenberg, "Rethinking rfid: Awareness and control for interaction with rfid systems," in *Proceedings of the SIGCHI Conference on Human Factors in Computing Systems*, ser. CHI '10. New York, NY, USA: ACM, 2010, pp. 2307–2316. [Online]. Available: http://doi.acm.org/10.1145/1753326.1753674

[6] *M24SR04: 4-Kbit Dynamic NFC / RFID tag with NFC Forum Tag Type 4 and I2C interface*, STMicroelectronics, November 2014. [Online]. Available: http://www.st.com

[7] *AS3953A: 14443 High Speed Passive Tag Interface*, AMS, June 2012. [Online]. Available: http://www.AMS.com

[8] A. Dehennis, M. Mailand, D. Grice, S. Getzlaff, and A. Colvin, "A near-field-communication (nfc) enabled wireless fluorimeter for fully implantable biosensing applications," in *Solid-State Circuits Conference Digest of Technical Papers (ISSCC), 2013 IEEE International*, Feb 2013, pp. 298–299.

[9] A. Sample, D. Yeager, P. Powledge, A. Mamishev, and J. Smith, "Design of an rfid-based battery-free programmable sensing platform," *Instrumentation and Measurement, IEEE Transactions on*, vol. 57, no. 11, pp. 2608–2615, Nov. 2008.

[10] (2015, January). [Online]. Available: http://www.openpcd.org/

[11] A. Dementyev, J. Gummeson, D. Thrasher, A. Parks, D. Ganesan, J. R. Smith, and A. P. Sample, "Wirelessly powered bistable display tags," in *Proceedings of the 2013 ACM international joint conference on Pervasive and ubiquitous computing*. ACM, 2013, pp. 383–386.

[12] D. Yeager, P. Powledge, R. Prasad, D. Wetherall, and J. Smith, "Wirelessly-charged uhf tags for sensor data collection," in *RFID, 2008 IEEE International Conference on*, april 2008, pp. 320 –327.

[13] A. Sample, J. Braun, A. Parks, and J. Smith, "Photovoltaic enhanced uhf rfid tag antennas for dual purpose energy harvesting," in *RFID (RFID), 2011 IEEE International Conference on*, April 2011, pp. 146–153.

[14] F. C. C. (FCC). (2011, January, 31) Title 47: Telecommunication. www.fcc.gov. [Online]. Available: http://www.fcc.gov/

[15] A. Christ, M. Douglas, J. Roman, E. Cooper, A. Sample, B. Waters, J. Smith, and N. Kuster, "Evaluation of wireless resonant power transfer systems with human electromagnetic exposure limits," *Electromagnetic Compatibility, IEEE Transactions on*, vol. 55, no. 2, pp. 265–274, April 2013.

[16] A. Sample, B. Waters, S. Wisdom, and J. Smith, "Enabling seamless wireless power delivery in dynamic environments," *Proceedings of the IEEE*, vol. 101, no. 6, pp. 1343–1358, June 2013.

[17] "http://nfc-wisp.wikispaces.com/."